# Aggregation of ZnO Nanorods into Films by Oriented Attachment

**Yugang Zhang,* Fang Lu, Zhenyang Wang, and Lide Zhang***

*Key Laboratory of Materials Physics, Anhui Key Lab of Nanomaterials and Nanotechnology Institute of Solid State Physics, Chinese Academy of Sciences, Hefei 230031, People's Republic of China*

*Received: October 23, 2006; In Final Form: January 7, 2007*

Highly oriented and densely packed ZnO films of nanorod arrays are formed free of substrate via a chemical vapor deposition (CVD) route. The resulting films are composed of single-crystal ZnO nanorods, which grow along their *c*-axis paralleling each other. The ZnO nanoclusters form first in the highly saturated vapor environment, followed by preferential growth along their [0001] directions to produce nanorods via a vapor−solid (VS) growth process. During transferring, the nanorods aggregate into films by oriented attachment with assistance of $ZnCO_3$. Raman scattering studies confirm that the ZnO nanorods are *c*-axis oriented and well-aligned as well as being of high-crystal quality. Room-temperature photoluminescence spectrum of such ZnO films exhibit a strong and narrow ultraviolet emission, which facilitates their potential applications in the future photoelectric nanodevices.

## 1. Introduction

With the ongoing miniaturization of microelectronics, one-dimensional (1D) nanoscale building blocks including nanotubes, nanowires, nanorods, and nanobelts have attracted extensive interest because of their remarkable physical and chemical properties and the potential to revolutionize broad areas of nanotechnology.[1] Among the various emerging 1D nanomaterials, zinc oxide (ZnO), with a direct wide band gap of 3.37 eV and a large exciton binding energy of 60 meV at room temperature, is one of the most promising functional semiconductor materials, which exhibits considerable properties including near-UV emission, optically transparent electrical conductivity, and piezoelectricity.[2] So far, plentiful 1D ZnO nanostructures, such as nanowires, nanotubes, and nanobelts, have been synthesized by various methods.[3] Furthermore, well-aligned ZnO nanowire/nanorod arrays demonstrating superior optical[4] and field emission properties[5] are proposed to be applied for UV lasers and field-emission displays, which stimulates further investigation for the controlled growth and the correlative mechanism studies of ZnO nanowire/nanorod arrays.

Currently, synthetic methodologies developed for alignment of 1D building blocks can be generally divided into two categories: (1) growth and postalignment (GPA), such as those adopting electric field,[6] fluid flow,[7] and Langmuir−Blodget technique,[8] and (2) coupled growth and alignment (CGA), such as catalyst-guided and template-assisted methods.[9] Up to now, various CGA strategies have been employed for the fabrication of well-aligned ZnO nanowire/nanorod arrays, such as vapor transport and condensation,[10] metal vapor deposition,[11] metal-organic source vapor deposition,[12] template-assisted growth,[13] buffer-layer-precoated route,[14] and laser-ablation methods.[15] However, so far, few studies have been centered on the GPA strategy for the synthesis of ZnO nanorod arrays.

In this work, highly oriented and densely packed ZnO films of nanorod arrays are formed free of substrate via GPA strategy. We demonstrate that the growth of the ZnO films is initiated by the formation of ZnO nanoclusters in the highly saturated vapor environment, followed by preferential growth along their [0001] directions to produce nanorods via a vapor−solid (VS) growth process. $ZnCO_3$ is responsible for the sequence of the aggregation nanorods into films by oriented attachment. Raman scattering studies confirm that the ZnO nanorods are *c*-axis oriented and well-aligned as well as being of high-crystal quality. Meanwhile, the room-temperature photoluminescence spectrum of such ZnO films exhibits a strong and narrow ultraviolet emission, which facilitates their potential applications in the future photoelectric nanodevices.

## 2. Experimental Section

The strategy utilized for the growth of ZnO films of nanorod arrays was carried out in a horizontal tube furnace with a gas supply system. A powder mixture of ZnO and graphite (molar ratio 1:1) was loaded in a ceramic boat and was put in the middle side of the ceramic tube. Additionally, the $ZnCO_3$ powders (99.999%) were loaded in another ceramic boat, which was placed on the downstream side. The whole system was heated at a rate of 30 °C/min from room temperature. High-purity Ar at a flow rate of 50 sccm was sent through the system. Once the temperature was raised to 950 °C, oxygen was switched on at a flow rate of 2 sccm. After heating at 1150 °C for 60 min, the system was cooled to room temperature. Pieces of yellow, fluffy products were found above the downstream side of the $ZnCO_3$ powder, where the temperature was 400−450 °C. The products had no adhesion with the deposition zone and they can be easily taken away from the boat.

The products were collected for characterization by field emission scanning electron microscopy (FE-SEM, Sirion 200), X-ray diffraction (XRD, Philips X'Pert, Cu Kα line: 0.15419 nm), and high-resolution transmission electron microscopy (HRTEM) (JEOL-2010). Raman and photoluminescence (PL) spectra were recorded using LABRAM-HR Micro-Raman spectrometer (Jobin-Yvon) excited with the 514.5-nm $Ar^+$ laser or a 325 He−Cd laser.

* To whom correspondence should be addressed. E-mail: ygzhang@issp.ac.cn (Y. Z.); ldzhang@issp.ac.cn (L. Z.).

10.1021/jp066956z CCC: $37.00 
Published on Web 03/03/2007

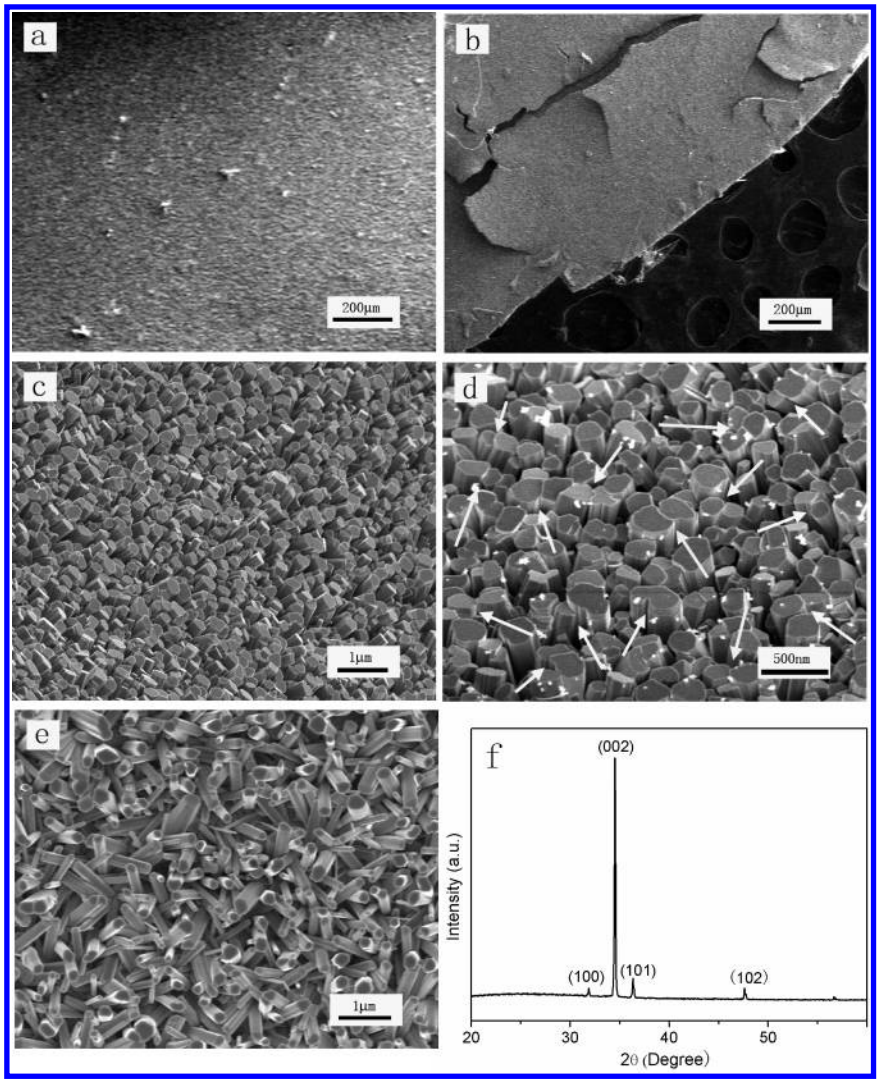


**Figure 1.** Low-magnification SEM images of (a) center and (b) edge of the as-synthesized films. (c−d) High-magnification SEM images of a. (e) SEM image of products obtained without $ZnCO_3$. (f) XRD pattern of the as-synthesized films.

## 3. Results and Discussion

**3.1. Structure Characterization.** According to the SEM observation, the resulting samples are close-packed films. The central part of the product is intact film with area up to several $mm^2$ (as shown in Figure 1a). Figure 1b shows the edge of the products, where the film is fractured into some small fragments. As shown in Figure 1c, the film is well-aligned with densely packed arrays, which are made up of straight nanorods with diameters ranging from 150 to 250 nm. In addition, the nanorods are attached to each other along their side surfaces (indicated by the white arrows in Figure 1d).

Figure 1f gives the corresponding XRD pattern of the films of nanorod arrays, which confirms that the nanorods are wurtzite-structured ZnO, compared with standard diffraction of wurtzite ZnO powders (JCPDS Card 36-1451). The very strong peak of the pattern corresponds to the {0002} plane, which indicates that the ZnO films are highly preferentially oriented along the *c*-axis. This is in good agreement with the above SEM observations.

The microstructures of the as-synthesized ZnO nanorods were further studied using TEM. Figure 2a shows a typical TEM image of a single nanorod with diameter about 200 nm, which was gently transferred onto a copper grid by ultrasonication. The HRTEM image in Figure 2b indicates that the nanorod is a single-crystal structure, according to which, it can be observed that the nanorod preferentially grows along the ⟨0001⟩ direction. The inset in Figure 2b gives the corresponding selected area electron diffraction (SAED) pattern, which further confirms the nanorod is single-crystalline and grows along its *c*-axis.

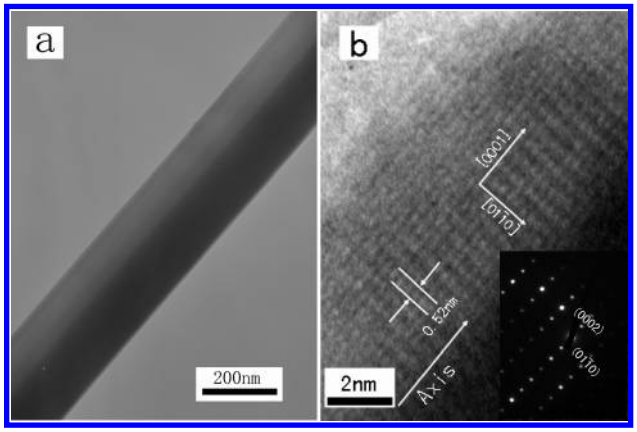


**Figure 2.** (a) TEM image of a single nanorod. (b) HRTEM image of a nanorod and its corresponding selected area electron diffraction pattern (inset).

**3.2. Growth Mechanism.** According to the above, it is proposed that the growth of ZnO films of nanorod arrays may

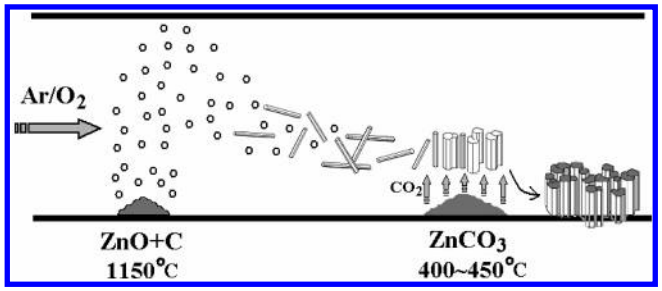


**Figure 3.** Schematic illustration for the growth mechanism of the ZnO films of nanorod arrays.

proceed in three steps, namely, nucleation, 1D growth, and self-aggravation into films of nanorod arrays, as illustrated in Figure 3.

First, at high-temperature zone, $ZnO_x$ ($0 \leq x < 1$) vapor is produced by reactions of ZnO powder with graphite. The vaporized $ZnO_x$ homogenously nucleate to form ZnO clusters in $Ar/O_2$ atmosphere. As is well-known, for ZnO nanocrystals, the preferential crystal growth along the ⟨0001⟩ direction is energetically favorable, which will finally result in the formation of ZnO nanorods.[3,16] In the course of transferring, the degree of supersaturation of ZnO is increasing together with the decreasing of the temperature, which leads the ZnO nanoclusters to preferentially grow into one-dimensional nanostructures (namely, the ZnO nanorods), since ZnO is a kind of anisotropic crystal and polar plane {0001} that has higher surface energy than that of the low-index nonpolar surfaces, such as {2-1-10} and {01-10}.

The ZnO nanorods have tendencies to deposit because of their weights turning larger and larger during their growing up. However, in this work, there is an upward $CO_2$ flow, which is produced by decomposing the designed $ZnCO_3$ in the starting materials, to keep them floating in the atmosphere. It is the assistance action of $CO_2$ that leads the ZnO nanorods to have chances to adjust their axes directions assembling into films by oriented attachment.[17] Up to now, various self-assembly processes based on different driving mechanisms have been reported.[18] Among which "oriented attachment" has attracted much attention as an effective mechanism for fabricating various kinds of nanostructures. Penn and Banfield first demonstrated that oriented attachment was an important growth process when aggregates of nanocrystalline titania particles coarsen under hydrothermal conditions.[17a] This mechanism is based on self-assembly primary nanoscale building blocks (i.e., nanoparticles) followed by spontaneous adjustment and lattice fusion of the adjacent crystallographic planes, in an ideal case of which the nanoscale building blocks are free to move in, for example, liquid or gas environments. During the subsequential transferring, building blocks of the films, that is, nanorods, grow long in length, since they could not become larger in diameter because of being confined by each other. When there is no flow upward, the films will drop down.

To validate our proposition, we prepared samples following the same process except that there is no $ZnCO_3$ adopted in the starting materials. According to the SEM observations (seen in Figure 1e), the nanorods are randomly oriented. Most of them are isolated from each other, which is quite different from the above-mentioned aligned nanorod arrays. This indicates that the designed $ZnCO_3$ assisting growth system does provide a crucial environment where the nanorods can be attached to each other along their side surfaces. However, in this work, the growth of the ZnO films was carried out in 60 min, while the $ZnCO_3$ powder can decompose completely within about 20 min even

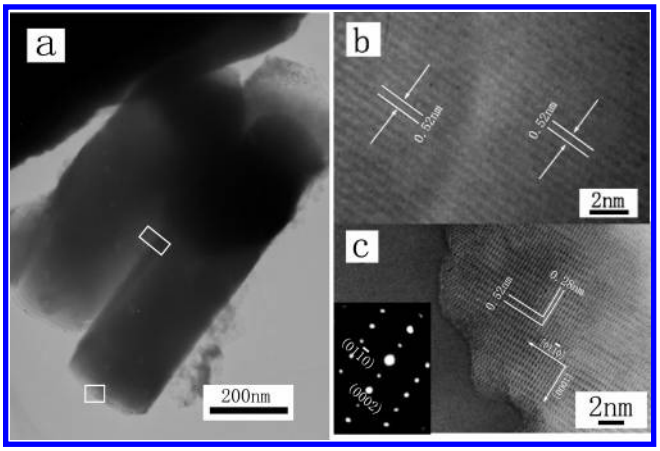


**Figure 4.** (a) TEM image of two coupled nanorods prepared in 20 min. (b) HRTEM image of the attached part of the nanorods (marked by a white rectangle in a). (c) HRTEM image of the top of a nanorod (marked by a white square in a) and its corresponding selected area electron diffraction pattern (inset).

though a full boat of $ZnCO_3$ powder was used. To further study the role of the $CO_2$ during the growth of the films, we prepared another sample following the same method mentioned in the Experimental Section except that the designed time is 20 min. The SEM observation shows that the resulting sample is filmlike, which is also composed of aligned nanorods. However, according to the TEM examinations, these nanorods are shorter than those prepared in 60 min, but the diameters are almost the same (as shown in Figure 4a). Figure 4b gives the HRTEM image recorded from the attached part of two coupled nanorods (marked by a white rectangle in Figure 4a), according to which these two nanorods have parallel (0001) lattice fringes and these (0001) crystal planes are perpendicular to the axes of the nanorods. The inset in Figure 4c gives the SAED pattern of the top surface of a nanorod (marked by a white square in Figure 4a), which also confirms that the nanorod grows along ⟨0001⟩ direction. The corresponding HRTEM image (seen in Figure 4c) reveals that there are many "steps" on the growth frontier of the nanorod. In the following growth process, $ZnO_x$ molecules can be preferentially absorbed and incorporated into the crystal lattices of these "steps" of the nanorods, leading the nanorods to grow longer.

**3.3. Raman Scattering.** Raman scattering was performed at room temperature to investigate the crystal quality and vibration properties of the ZnO films of nanorod arrays. Wurtzite ZnO belongs to the $C_{6v}^4$ space group, with two formula units per primitive cell. At the Γ point of the Brillouin zone, the normal lattice vibration modes are predicted on the basis of group theory: $\Gamma_{opt} = A_1(z) + 2B_1 + E_1(x, y) + 2E_2$,[19] among which $E_1$, $E_2$, and $A_1$ are the first-order Raman active modes, and $B_1$ is forbidden. Meanwhile, the $E_1$ and $A_1$ modes split into longitudinal optical (LO) and transverse optical (TO) components. Figure 5a and b gives the nonresonant Raman spectra of the as-synthesized ZnO films of nanorod arrays and the randomly oriented ZnO nanorods, respectively. It can be seen that all the modes are attributed to the vibration of wurtzite ZnO crystal,[20] and the identification of these modes is marked in Figure 5. Compared with the modes of the randomly oriented ZnO nanorods, the TO modes are absent in the spectrum of ZnO films, which might result from the special angle between the wave vector of photons and the *c*-axial direction of the ZnO nanorods.[21] In our experiment, the incident laser light was parallel to the *c*-axes of the ZnO nanorods and Raman signal was recorded in the backscattering geometry. According to the Raman selection rules, only $E_2$ and $A_1$(LO) modes are allowed,

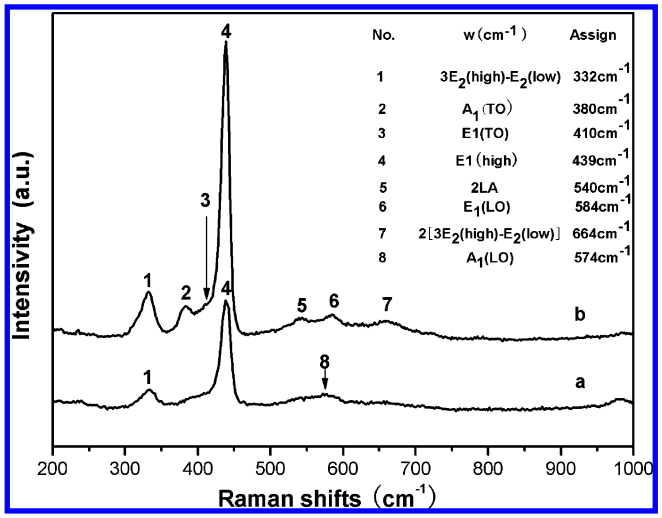


**Figure 5.** Raman spectra of (a) ZnO films of nanorod arrays and (b) randomly oriented nanorods.

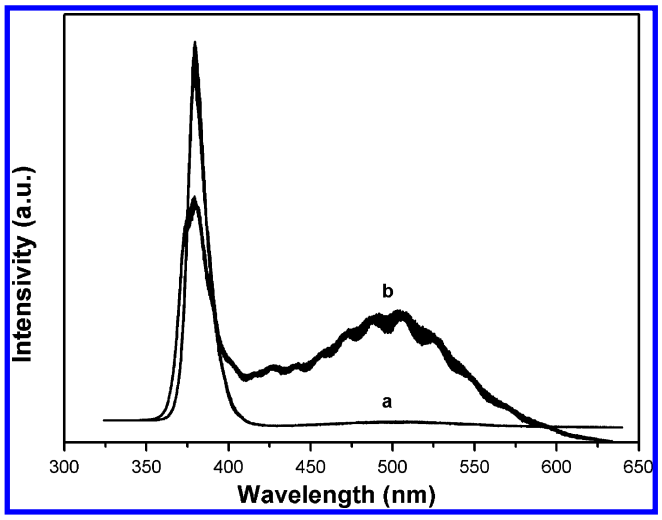


**Figure 6.** Room-temperature PL spectra of (a) ZnO films of nanorod arrays and (b) randomly oriented nanorods.

while the $A_1$(TO) and $E_1$(TO) are forbidden. Thus, the absence of the TO modes in the measurements further confirms that the ZnO nanorods are highly *c*-axis oriented.

**3.4. Photoluminescence.** The optical properties of the ZnO films of nanorod arrays and the randomly oriented ZnO nanorods were studied at room temperature using a PL spectrum excited with a 325-nm He−Cd laser. The results are shown in Figure 6. The films show a strong sharp UV emission at ∼378 nm (3.28 eV), which is attributed to the near-band-edge emission. The full width at half-maximum (fwhm) of this emission peak is estimated to be 100 meV, which is smaller than the value for ZnO nanowire arrays (120 meV) grown on anodic aluminum[22] or silicon substrate by the CVD method[10a] or ZnO nanowires (110 meV) grown on m-sapphire substrate by the carbothermal method.[23] This narrow fwhm proves that the films of ZnO nanorod arrays are of high-crystal quality. Besides the UV emission, the randomly oriented ZnO nanorods show a broad green emission centered at 500 nm, which is generally referred to as a deep-level or trap-state emission. To explain the green emission, various models, such as the involvement of O vacancies,[24] interstitial O,[25] Zn vacancies, and Zn interstitials,[26] have been proposed. Recently, Hsu et al. showed that the intensity of the UV/green emission had a maximum (minimum) parallel (perpendicular) to the *c*-axis of the ZnO nanowire and proposed that the green emission was mainly generated and emitted from the side walls of the nanowires.[27] In our experiment, the emission was collected from normal to the sample surface and there was more UV emission along the *c*-axis from the side surface self-attached nanorods. This may be the reason why the green emission does not appear in the well-aligned nanorod arrays.

## 4. Conclusions

In summary, ZnO films of nanorod arrays have been synthesized free of substrate via GPA strategy by a CVD method. The ZnO nanorods are formed first, followed by the aggregation along the side surfaces of nanorods into well-aligned and densely packed films with assistance of the designed $CO_2$ flow. The ZnO nanorods are well-aligned and *c*-axis oriented with high-crystal quality, which is further confirmed by Raman scattering studies. The PL measurements show that the ZnO films have a strong and narrow ultraviolet emission, which facilitates potential applications in future photoelectric nanodevices. This GPA technique will be constructive to better understand the behavior of ZnO nanoscale building blocks in a vapor-phase synthetic system. It represents an effective strategy for direct assembly of one-dimensional structure arrays of some other materials free of substrate for support.

**Acknowledgment.** This work was financially supported by the National Major Project of Fundamental Research: Nanomaterials and Nanostructures (Grant No. 2005CB23603), the Special fund for President Scholarship, Chinese Academy of Science, and the National Natural Science Foundation of China (Grant No. 90406008).

## References and Notes

(1) Hu, J. T.; Odom, T. W.; Lieber, C. M. *Acc. Chem. Res.* **1999**, *32*, 435.

(2) See, for review: Özgür, Ü.; Alivov Ya, I.; Liu, C.; Teke, A.; Reshchikov, M. A.; Dogan, S.; Avrutin, V.; Cho, S. -J.; Morkoçd, H. *J. Appl. Phys.* **2005**, *98*, 041301.

(3) See, for review: Wang, Z. L. *J. Phys.: Condens. Matter* **2004**, *303*, R829.

(4) Huang, M. H.; Mao, S.; Feick, H. N.; Yan, H. Q.; Wu, Y. Y.; Kind, H.; Weber, E.; Russo, R.; Yang, P. D. *Science* **2001**, *292*, 1897.

(5) Cui, J. B.; Daghliam, C. P.; Gibson, U. J.; Pusche, R.; Geithner, P.; Ley, L. *J. Appl. Phys.* **2005**, *97*, 044315.

(6) Smith, P. A.; Nordquist, C. D.; Jackson, T. N.; Mayer, T. S.; Martin, B. R.; Mbindyo, J.; Mallouk, T. E. *Appl. Phys. Lett.* **2000**, *77*, 1399.

(7) Huang, Y.; Duan, X; Wei, Q; Lieber, C. M. *Science* **2001**, *291*, 630.

(8) Kim, F.; Kwan, S.; Alkana, J.; Yang, P. D. *J. Am. Chem. Soc.* **2001**, *123*, 4360.

(9) Xia, Y.; Yang, P.; Sun, Y.; Wu, Y.; Mayers, B.; Gates, B.; Yin, Y.; Kim, F.; Yan, H. *Adv. Mater.* **2003**, *15*, 353.

(10) (a) Geng, C.; Jiang, Y.; Yao, Y.; Meng, M.; Zapien, J. A.; Lee, C. S.; Lifshitz, Y.; Lee, S. T. *Adv. Funct. Mater.* **2004**, *14*, 589. (b) Park, W. I.; Yi, G. C.; Kim, M.; Pennycook, S. L. *Adv. Mater.* **2002**, *14*, 1841.

(11) Tseng, Y. K.; Huang, C. J.; Cheng, H. M.; Lin, I. N.; Liu, K. S.; Chen, I. C. *Adv. Funct. Mater.* **2003**, *13*, 812.

(12) Park, W. L.; Kim, D. H.; Jung, S. W.; Yi, G. C. *Appl. Phys. Lett.* **2002**, *80*, 4232.

(13) Zheng, M. J.; Zhang, L. D.; Li, G. H.; Shen, W. Z. *Chem. Phys. Lett.* **2002**, *363*, 123.

(14) (a) Greene, L. E.; Law, M.; Goldberger, J.; Kim, F.; Johnson, J. C.; Zhang, Y. F.; Saykally, R. J.; Yang, P. D. *Angew. Chem., Int. Ed.* **2003,** *42*, 3031. (b) Vayssieres, L. *Adv. Mater.* **2003**, *15*, 464.

(15) Lorenz, M.; Kaidashev, E. M.; Rahm, A.; Nobis, Th.; Lenzner, J.; Wagner, G.; Spemann, D.; Hochmuth, H.; Grundmann, M. *Appl. Phys. Lett.* **2005**, *86*, 143113.

(16) (a) Laudise, R. A.; Ballma, A. A. *J. Phys. Chem.* **1960**, *64*, 688. (b) Fan, H. J.; Bertram, F.; Dadgar, A.; Christen, J.; Krost, A.; Zacharias, M. *Nanotechnology* **2004**, *15*, 1401.

(17) (a) Penn, R. L.; Banfield, J. F. *Science* **1998**, *281*, 969. (b) Zhang, H.; Banfield, J. F. *Nano Lett.* **2004**, *4*, 713. (c) Tang, Z.; Kotov, N. A.;

Giersig, M. *Science* **2002**, *297*, 237. (d) Ribeiro, C.; Lee, E. J. H.; Giraldi, T. R.; Varella, J. A.; Longo, E.; Leite, E. R. *J. Phys. Chem. B* **2004**, *108*, 15612.

(18) (a) Yang, H. G.; Zeng, H. C. *J. Phys. Chem. B* **2004**, *108*, 3492. (b) Yin, Y.; Rioux, R. M.; Erdonmez, C. K.; Hughes, S.; Somorjai, G. A.; Alivisatos, A. P. *Science* **2004**, *304*, 711. (c) Park, S.; Lim, J. H.; Chung, S. W.; Mirkin, C. A. *Science* **2004**, *303*, 348. (d) Pacholski, C.; Kornowski, A.; Weller, H. *Angew. Chem.* **2002**, *114*, 1234.

(19) Scott, J. F. *Phys. Rev. B* **1970**, *2*, 1209.

(20) Damen, T. C.; Porto, S. P.; Tell, B. *Phys. Rev.* **1966**, *142*, 570.

(21) (a) Kaschner, A.; Haboeck, U.; Strassburg, M.; Kaczmarczyk, G.; Hoffmann, A.; Thomsen, C.; Zeuner, A.; Alves, H. R.; Hofmann, D. M.; Meyer, B. K. *Appl. Phys. Lett.* **2002**, *80*, 1909. (b) Zhang, Y.; Jia, H.; Wang, R.; Chen, C.; Luo, X.; Yu, D.; Lee, C. *Appl. Phys. Lett.* **2003**, *83*, 4631.

(22) Jie, J.; Wang, G.; Wang, Q.; Chen, Y.; Han, X.; Wang, X.; Hou, J. *J. Phys. Chem. B* **2004**, *108*, 11976.

(23) Ng, H.; Chen, B.; Li, J.; Han, J.; Meyyappan, M.; Wu, J.; Li, S.; Haller, E. *Appl. Phys. Lett*. **2003**, *82*, 2023.

(24) Vanheusden, K.; Warren, W.; Seager, C.; Tallant, D.; Voigt, J. *J. Appl. Phys.* **1996**, *79*, 7983.

(25) Liu, M.; Kitai, A.; Mascher, P. *J. Lumin.* **1992**, *54*, 35.

(26) Bylander, E. *J. Appl. Phys.* **1978**, *49*, 1188.

(27) Hsu, N.; Hung, W.; Chen, Y. *J. Appl. Phys.* **2004**, *96*, 4671.